Electronic Supplementary Information

$ZnIn_2S_4$ thin films with hierarchical porosity for photocatalysis

Marco Sigl,[a] Melissa Egger,[a] Fernando Warchomicka,[b] Daniel Knez,[c] Martina Dienstleder,[d] Heinz Amenitsch,[e] Gregor Trimmel[a] and Thomas Rath[a,*]

[a] Institute for Chemistry and Technology of Materials, NAWI Graz, Graz University of Technology, Stremayrgasse 9, 8010 Graz, Austria.

[b] Institute of Materials Science, Joining and Forming, Graz University of Technology, Kopernikusgasse 24, 8010 Graz, Austria.

[c] Institute of Electron Microscopy and Nanoanalysis, Graz University of Technology Steyrergasse 17, 8010 Graz, Austria.

[d] Austrian Centre for Electron Microscopy and Nanoanalysis, Steyrergasse 17, 8010 Graz, Austria.

[e] Institute of Inorganic Chemistry, NAWI Graz, Graz University of Technology, Stremayrgasse 9, 8010 Graz, Austria.

* thomas.rath@tugraz.at

Synthesis of zinc O-pentan-1-yl-dithiocarbonate (ZnXaC5)

First, we synthesized the potassium analogue, potassium O-pentyl-1-yl-dithiocarbonate (KXaC5), according to previous reports in literature as precursor for the zinc xanthate.[1,2] For the KXaC5 synthesis, 1.0 equiv. of potassium hydroxide (49.0 mmol) was added to 1.1 equiv. (55.0 mmol) of 1-pentanol. The mixture was cooled in an ice bath and 1.1 equiv. of CS_2 (55.0 mmol) were dropped into the mixture. The yellow slurry was stirred for 30 min and washed with diethyl ether. The product was collected by filtration and dried under vacuum overnight. The dried product was dissolved in acetone and re-precipitated in diethyl ether, followed by another filtration to obtain the pure, light-yellow product (yield = 55 %).

The synthesis of the zinc xanthate was also based on previous reports.[3–5] 1 equiv. of $ZnCl_2$ was dissolved in 24 mL of deion. water and 2.1 equiv. of the purified KXaC5 were dissolved in 36 mL of deion water. The potassium xanthate solution was added dropwise to the zinc chloride solution under vigorous stirring. A white precipitate formed immediately. The mixture was stirred for 2 h at room temperature and the white solid was filtrated and dried under vacuum overnight (yield = 93 %). ^{1}H NMR (300 MHz, $CDCl_3$ -7.26 ppm): δ = 4.98 (t, 2 H), 1.84 (m, 2 H), 1.39 (m, 4 H), 0.93 (t, 3 H) ppm.

FT-IR (ν / cm^{-1}): 2950, 2917, 2868, 2854, 1465, 1375, 1322, 1189, 1142, 1128, 1069, 1036, 1005, 940.

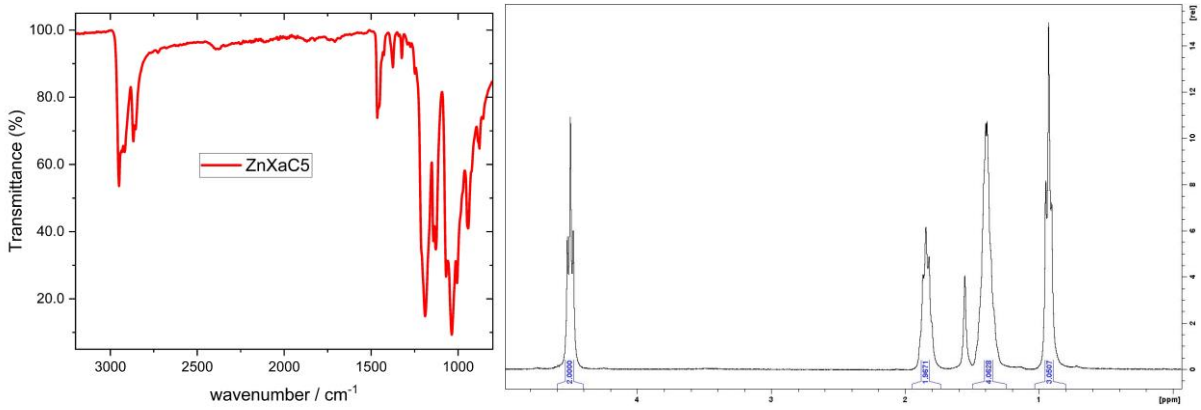

Fig. S1 *IR and ^{1}H NMR spectra of zinc O-pentan-1-yl-dithiocarbonate.*

Indium O-2,2-dimethylpenthan-3-yl dithiocarbonate

The indium xanthate was bought from Aglycon GmbH and recrystallized from chloroform/methanol. Aglycon synthesized the indium xanthate based on a previously published paper:[2]

Similar to the zinc xanthate, first the potassium analogue was synthesized. Potassium tert-butoxide (1.0 equiv.) was dissolved in THF in inert atmosphere. The solution was cooled to 0 °C, then 2,2-dimethyl-3-pentanol (1.1 equiv.) were slowly added. After stirring for a few minutes, CS_2 (1.1 equiv.) were added dropwise and the solution was stirred for about 5 hours. The reaction mixture was diluted with diethyl ether. The obtained solid was dried in vacuum and afterwards dissolved in acetone to separate insoluble side products. The acetone solution was concentrated by rotary evaporation and then the product was precipitated by addition of diethyl ether. The product was separated by filtration and dried under vacuum to give a white-yellowish powder.

Indium(III) chloride (1.0 equiv.) was dissolved in 300 mL of deion. water. To this solution, a solution of the potassium xanthate (3.2 equiv.) dissolved in 350 mL of deion. water was added dropwise under stirring. The reaction was allowed to stir for about 2.5 hours. The white residue was filtered and dried

in vacuum. The product was recrystallized from chloroform/methanol to a white powder, which was again dried in vacuum.

^{1}H NMR (300 MHz, $CDCl_3$ -7.26 ppm): δ 4.67 - 4.83 (m, 1 H), 1.67 – 1.84 (m, 2 H), 0.95 – 1.07 (m, 12 H).

FT-IR (ν / cm^{-1}): 2964, 2872, 1477, 1466, 1455, 1367, 1345, 1238, 1212, 1128, 1079, 1053, 1030, 1012, 951, 902.

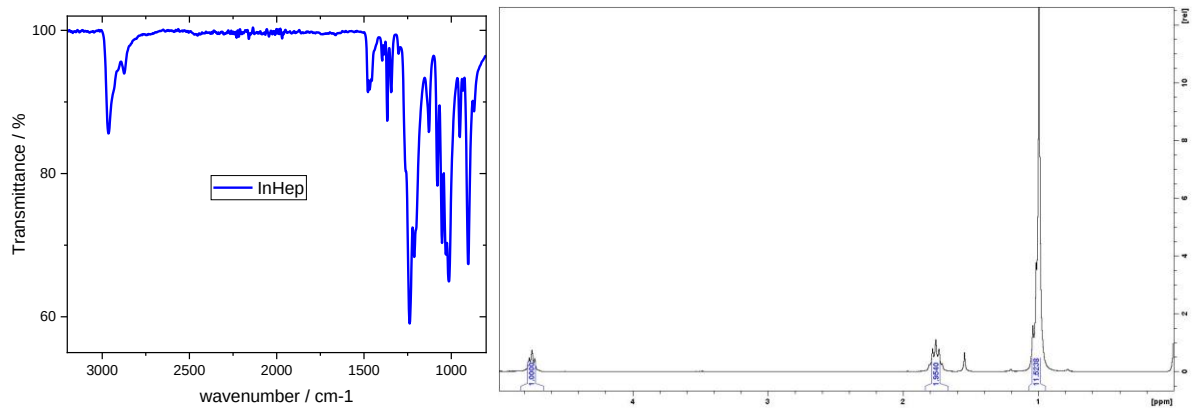

Fig. S2 *IR- and ^{1}H NMR spectra of indium O-2,2-dimethylpenthan-3-yl dithiocarbonate.*

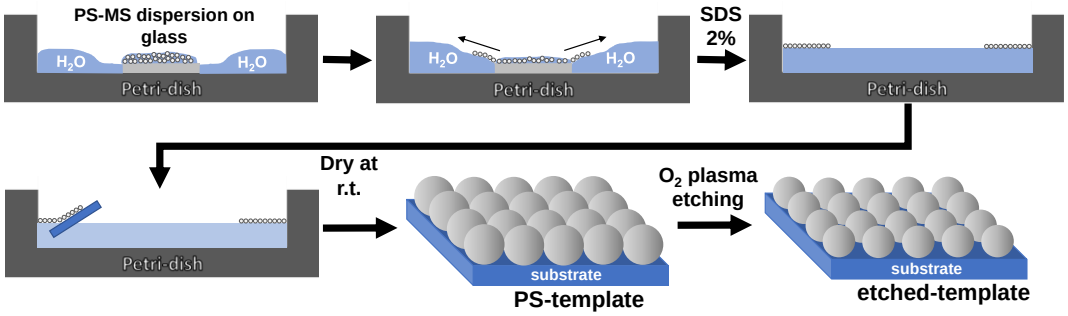

Fig. S3 *Schematic representation of the PS-MS preparation.*

PS-MS template preparation

Using an air/liquid interface as shown in **Fig. S3**, a polystyrene bead suspension in water/ethanol (Sigma Aldrich, latex beads; diameter: 0.3 µm) was put on a glass substrate placed in the middle of a petri dish. Deion. H_2O was added slowly until it overcame the surface tension of the glass substrate, and the PS-MS was rapidly dispersed on the water/air interface. By adding a surfactant, the beads are pushed to a tightly packed two-dimensional layer, which we transferred onto silicon substrates by simply lifting them up from the interface. By fulfilling the Bragg condition,[7] the PS-MS film shows a blue shimmering structural colour. This can be seen at the water/air interface as well as on the dried film on the silicon substrate.

To create space for the precursor solutions between the tightly packed spheres, we treated the PS-MS films with an O_2 plasma to isotropically reduce the sphere sizes. This provides a great way to homogeneously control the size of the beads and thus the later size of the macropores and the wall thicknesses as presented in Fig. S4 and Fig S14. After the O_2 plasma treatment, the template-films were infiltrated by a precursor solution containing the metal xanthates acting as zinc, indium, and sulfur sources for the formation of zinc indium sulfide.

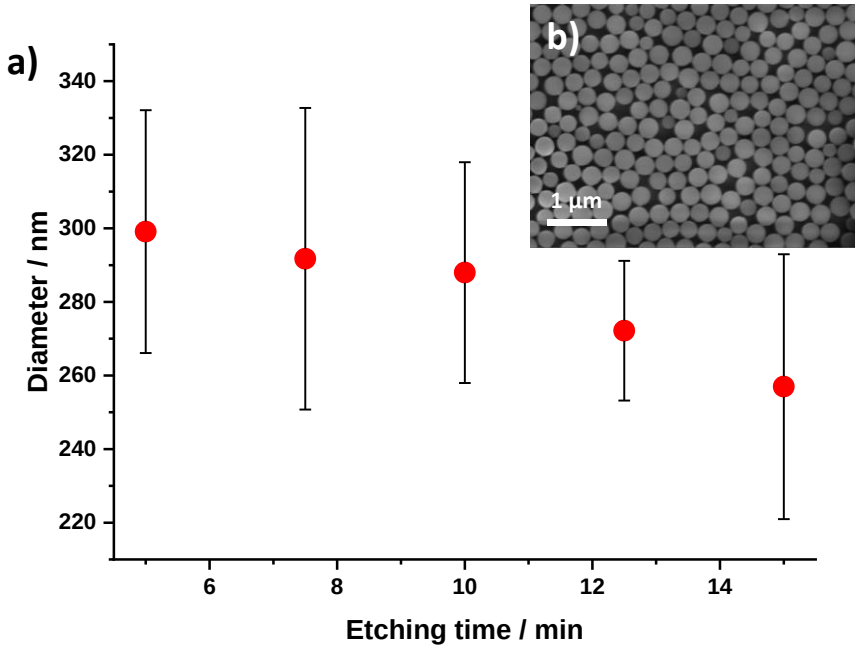

Fig. S4 *a) PS-MS diameters depending on the O_2 etching time; b) SEM image of PS-MS beads after 5 min in the O_2 plasma.*

Table S1: *Solvent mixtures for the xanthate precursor solutions*

solvent (mixture)	components	volume ratio
DCM	dichloromethane	1
EDE	ethanol:dichloromethane:ethanolamine	20:10:1
PDE	iso-propanol:dichloromethane:ethanolamine	4:2:1
PDE2	iso-propanol:dichloromethane:ethanolamine	20:10:1

Table S2 *Mass losses and decomposition temperature of the individual xanthate precursors and the 1:1.8 mixtures in the respective solvents*

compound	theoretical mass loss / %	observed mass loss / %	decomposition temperature at 5% mass loss / °C
InHep	76.4	76.0	140
ZnXaC5	75.1	74.6	126
DCM	76.1	76.0	112
EDE	76.1	79.4	92

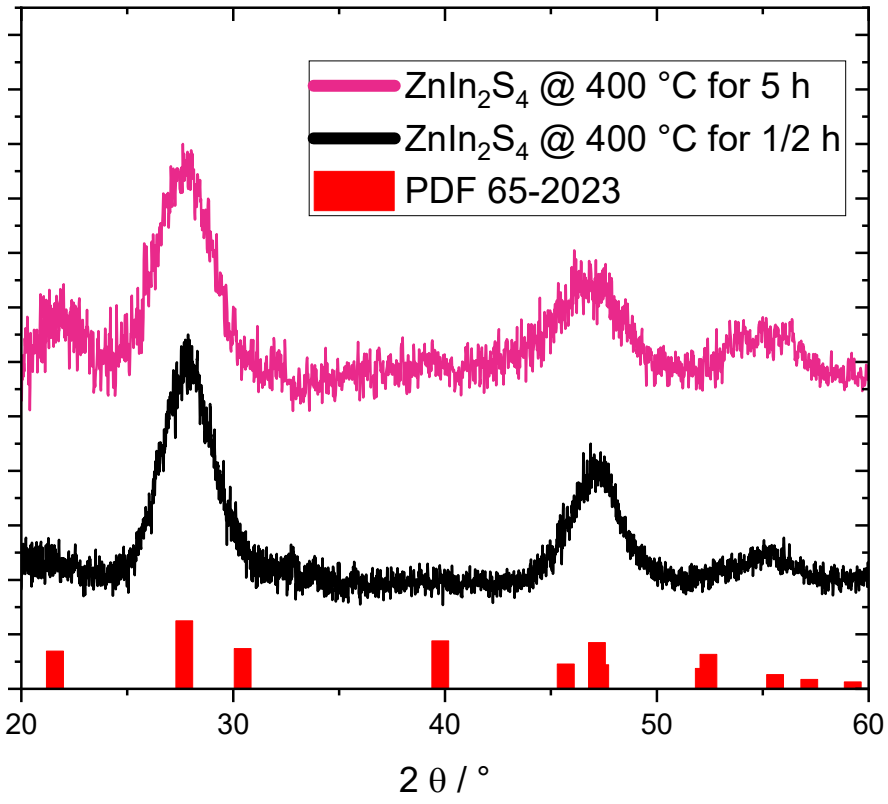

Fig. S5 *Diffractogram of $ZnIn_2S_4$ after 30 minutes annealing at 400 °C and after 5 h at 400 °C and the reference pattern for $ZnIn_2S_4$ (PDF 65-2023).*

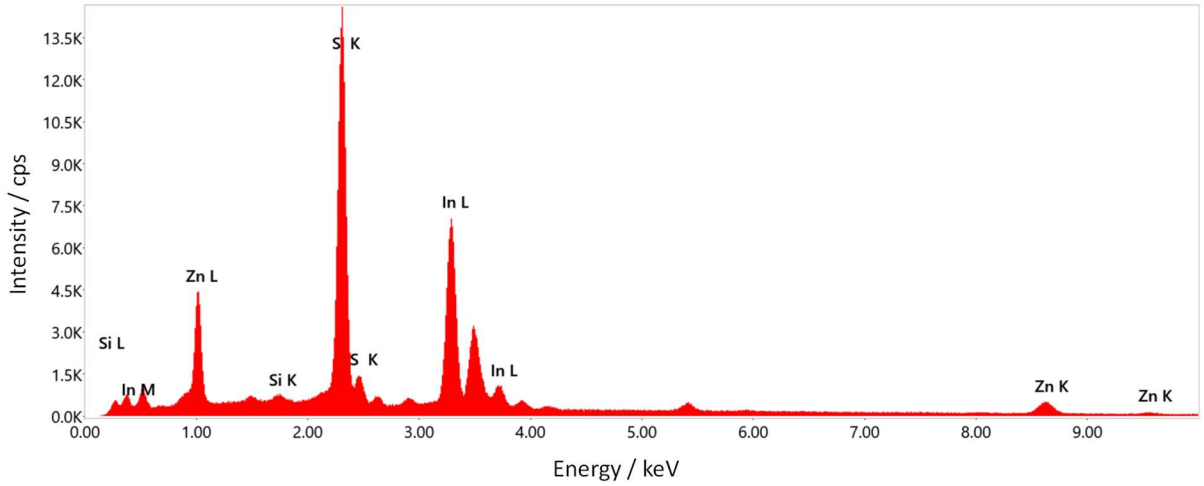

Fig. S6 *EDX spectrum of a $ZnIn_2S_4$ film (drop coated precursor solution) on a silicon substrate.*

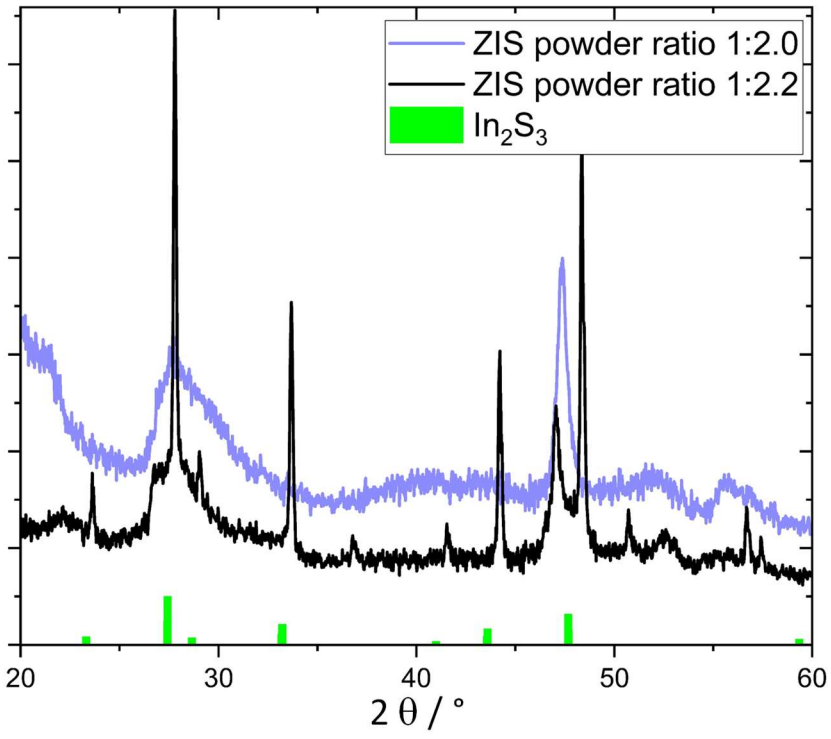

Fig. S7 *X-ray diffractogram of ZIS powder prepared from precursors used in a molar ratio of 1:2.2 and 1:2.0 (Zn:In), as well as In_2S_3 (COD 4000813) as reference pattern.*

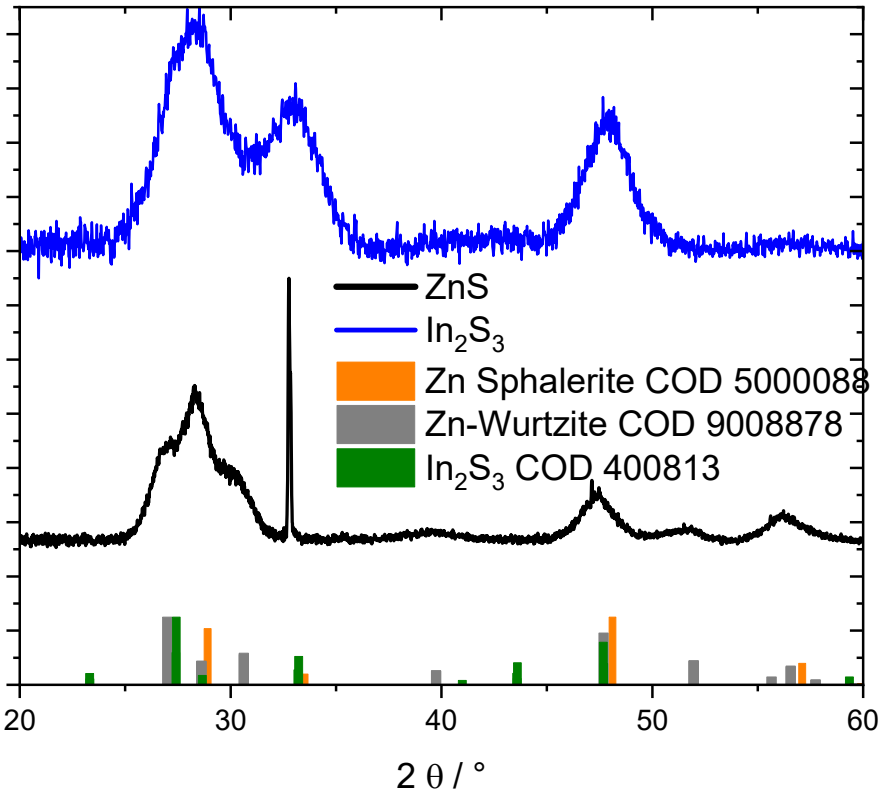

Fig. S8 *Diffractograms of individually converted zinc and indium sulfides. * In the ZnS diffractogram at 32.9 ° 2θ, a peak from the silicon substrate can be seen.*

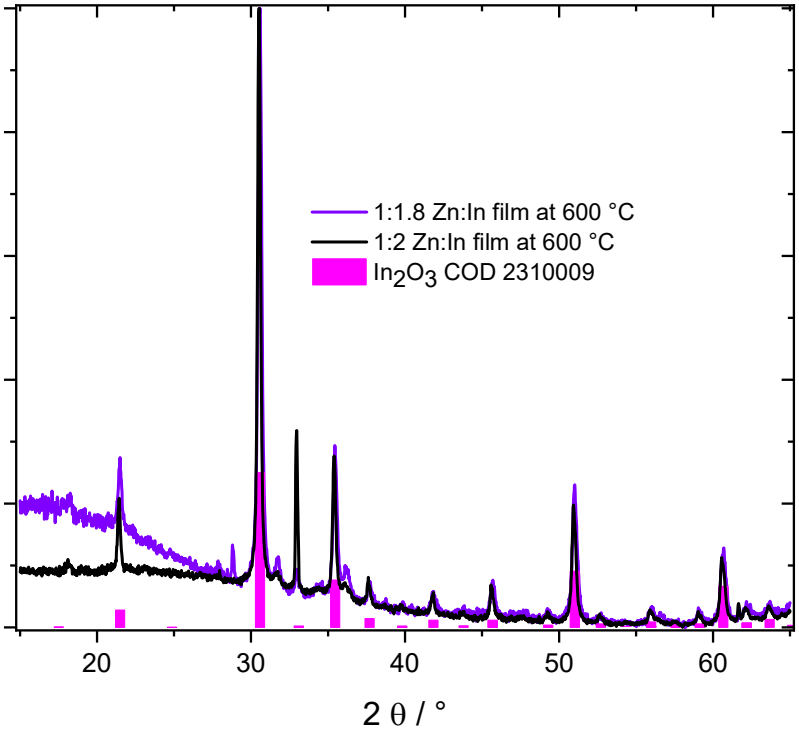

Fig. S9 *Diffractograms of $ZnIn_2S_4$ thin films after annealing at 600 °C 30 minutes.*

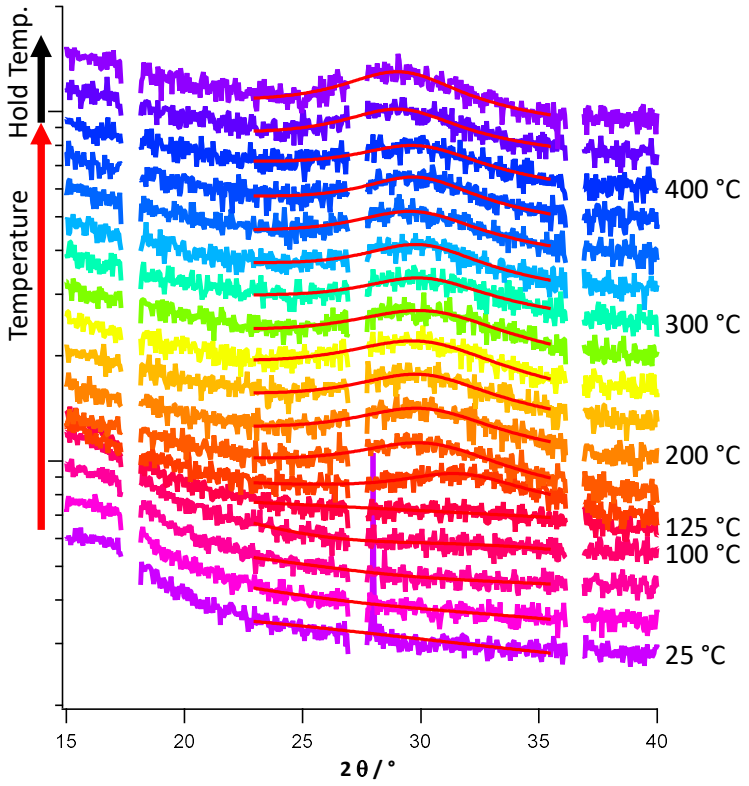

Fig. S10 *GIWAXS curves in 25 °C steps from 25 to 400 °C with fitted peaks (red lines). The curves are vertically shifted for better visibility.*

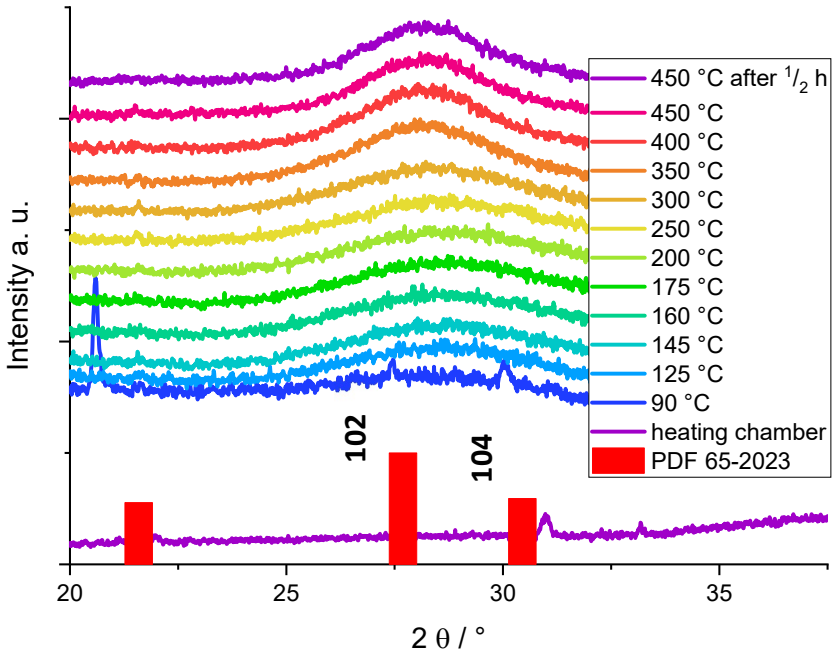

Fig. S11 *X-ray diffractograms over the course of the $ZnIn_2S_4$ formation (vertically shifted for better visibility).*

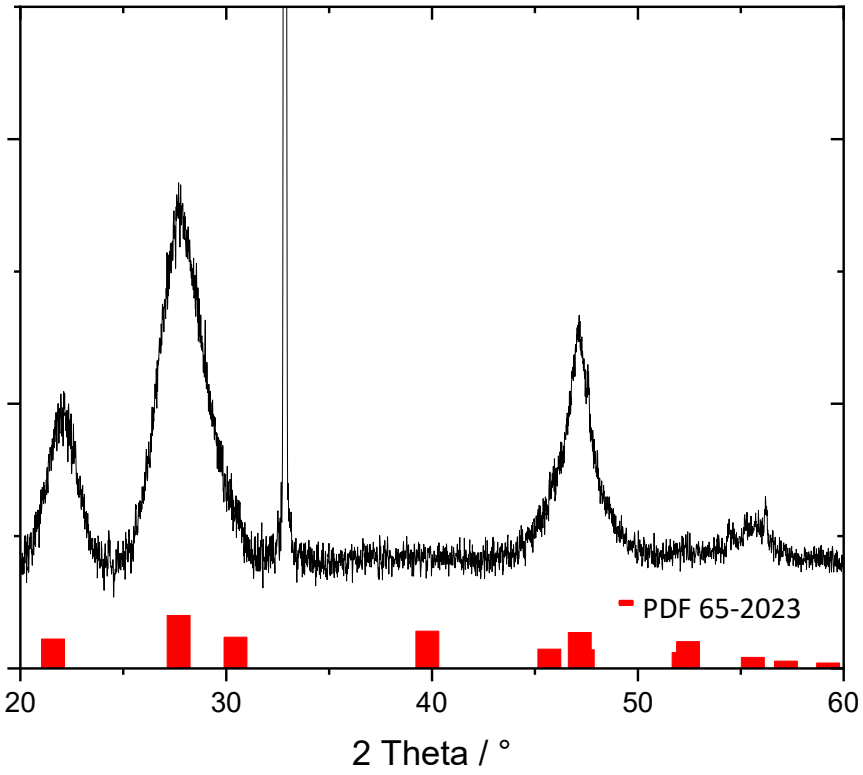

Fig. S12 *Diffractogram of $ZnIn_2S_4$ with the precursors diluted in PDE. * The narrow peak at 32.9 ° 2θ stems from the silicon substrate.*

Table S3 *Average macropore sizes of the structured thin films with different solvents and plasma etching time*

solvent mixture	O_2 etching time/ min	pore diameter / nm	wall thickness / nm
EDE	10	304 ± 43	48 ± 16
EDE	15	289 ± 48	61 ± 23
PDE1	10	331 ±48	35 ± 14
PDE1	15	313 ± 59	47 ± 16
PDE2	10	327 ± 38	22 ± 10
PDE2	15	299 ± 56	/**

** Because of irregular pore-formation and partial dissolution of the template, the wall thicknesses could not be reasonably measured.

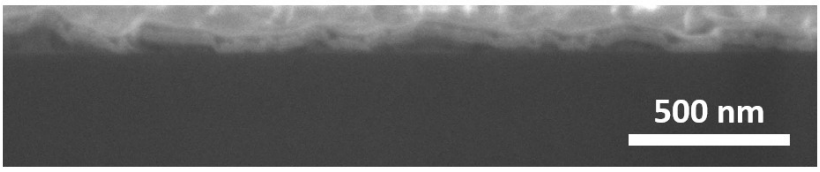

Fig. S13 *SEM cross section image of a structured $ZnIn_2S_4$ film on a silicon substrate prepared using EtOH:DCM:ETA (20:10:1) as solvent and 10 min O_2 plasma treatment of the PS-MS template.*

Preparation of the cross sections and characterization via SEM:

First, the samples were thinly coated with AuPd to create a visually observable demarcation during the SEM examination, as redeposition of sputtered material occurs during preparation with an IonMiller.

Cross sectioning was performed with a Gatan ILION model 693 broad ion beam miller with 6 kV acceleration voltage at -130 °C, from the backside. This means, the ion beam impact goes from the substrate side over to the layer side to generate a flat and curtaining free cross section.

SEM cross section images were recorded in a FEI Nova Nanolab200 (Thermo Fisher Scientific) equipped with a through-the-lens detector (TLD) at 2 kV and 0.21 nA.

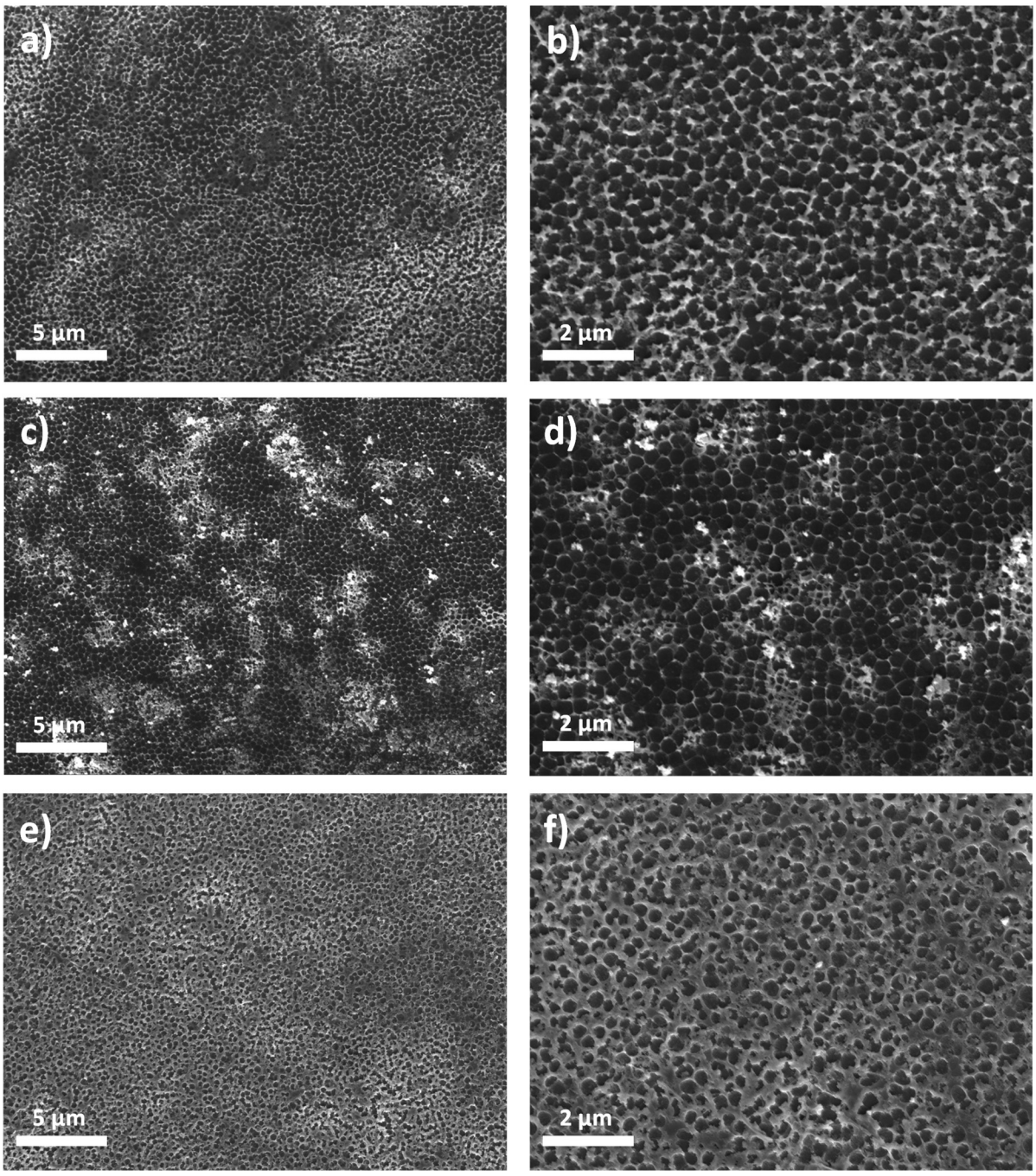

Fig. S14 *SEM images of a structured film prepared (a,b) from a iPrOH:DCM:EtA 4:2:1 (vol:vol:vol) precursor solution a) 10kx, b) 25 kx magnification and (c,d) a iPrOH:DCM:EtA 20:10:1 (vol:vol:vol) precursor solution with c) 10 kx and d) 25 kx magnification after 10 minutes in the O_2 plasma and (e,f) from a EtOH:DCM:EtA 20:10:1 (vol:vol:vol) precursor solution with e) 10 kx and f) 25 kx magnification after 15 minutes in the O_2 plasma.*

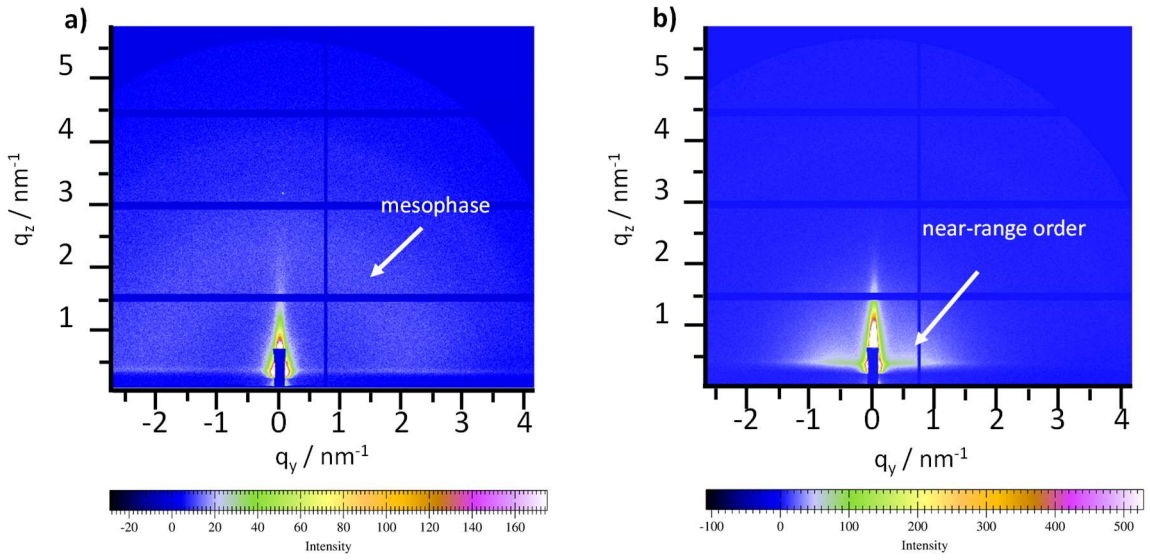

Fig. S15 *GISAXS patterns (a) at 145 °C and (b) 400 °C acquired during the heating run of the $ZnIn_2S_4$ planar film using the EDE mixture as solvent.*

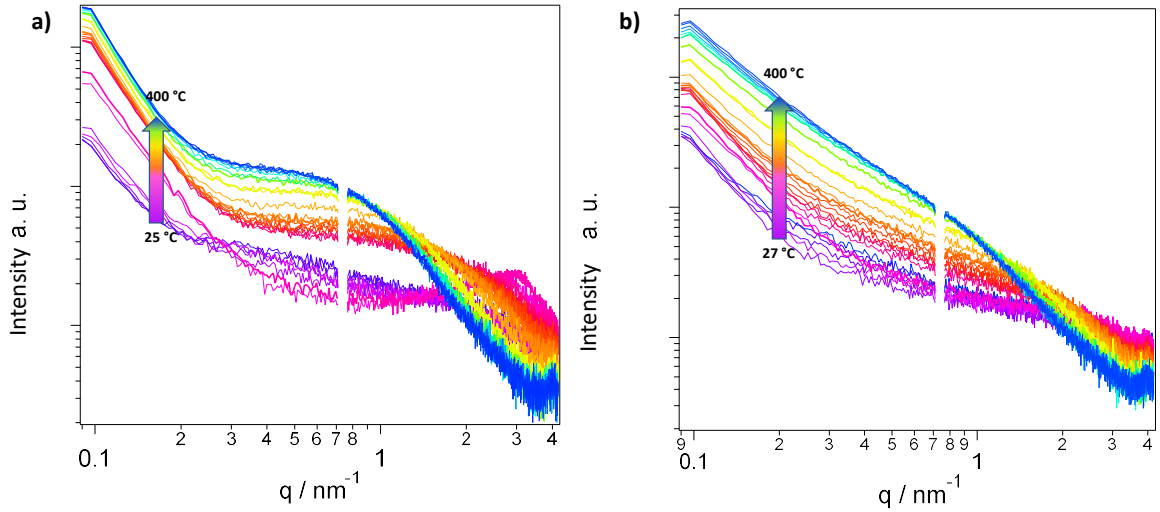

Fig. S16 *Horizontal line-cuts of a) planar EDE and b) structured EDE for chosen temperatures.*

Calculation of the invariant and correlation length

We calculated the GISAXS invariant $\bar{I}$ and the correlation length in the in-plane direction $\hat{I}_c$ (integration over q_{min} = 0.10 to q_{max} 4.18 nm^{-1}) as qualitative sensitive measure for changes in the films. $I(q_h)$ describes the scattering pattern and q_h the q-values in the horizontal direction.

$$\bar{I} = \int_{q_{min}}^{q_{max}} dq_h q_h^2 I(q_h)$$

$$\hat{I}_c = \frac{\pi}{\bar{I}} \int_{q_{min}}^{q_{max}} dq_h q_h I(q_h)$$

GISAXS data fitting

The GISAXS data was fitted according to the following equation:

$I_{calc}(q) = a * F(q) * S_{SHS}(q) + I_{Porod}(q) + BG$

- a describes an intensity scalar
- F(q) describes the form-factor scattering
- $S_{SHS}(q)$ describes the structure-factor contribution (Sticky hard sphere)
- $I_{Porod}(q)$ describes the Porod-contribution resulting from large scale aggregates
- BG describes the background

For the description of the Form-Factor, an analytic expression for polydisperse Schultz-distributed spheres is used. The structure factor contribution is described by a sticky hard sphere model. The used parameters for the function are illustrated in **Fig. S17**. More elaborated details to the fitting function and origin of the parameters are given in the publications of, Pontoni et al. (2003),[8] Sharma et al. (1977),[9] Kotlarchyk et al. (1988)[10] and Rigodanza et al. (2021).[11]

Fitting parameters:

Schematic

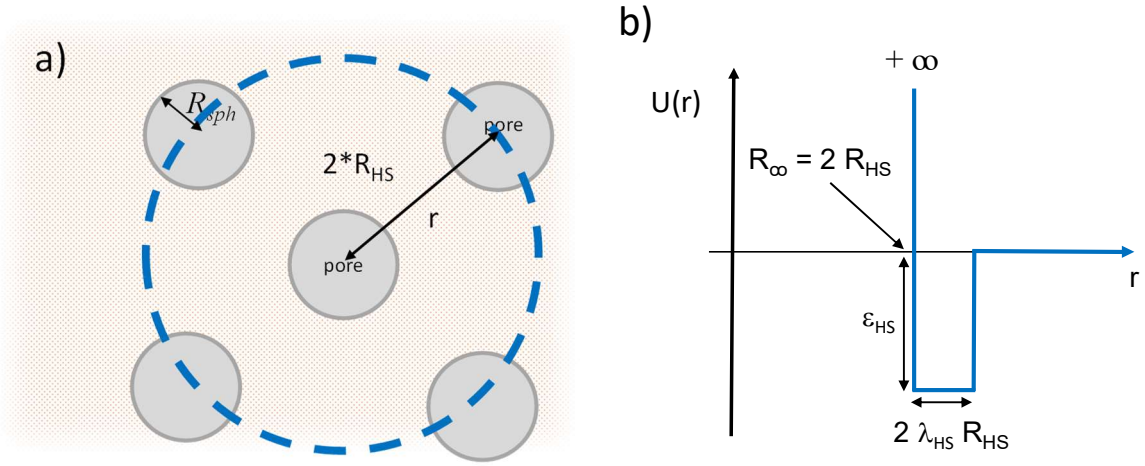

Fig. S17 *Schematic representation of a) the nanopores and b) the square-well potential where R_{sph} is the Schultz sphere radius and ε_{HS} and λ_{HS} describe the square-well depth and relative width.*

Table S4 *Fitting parameters with short description*

parameter	description
I_{sph}	scattering intensity
R_{sph}	Schultz sphere-radius (pore-sizes)
sig_{sph}	deviation of the pore sizes
R_{HS}	hard-sphere radius (pore-pore distances)
p_{HS}	particle volume fraction
λ_{hs}	relative potential well size, $\lambda_{hs} = 0.1$ ($\lambda = 1 + \lambda_{hs}$)
ε_{HS}	relative potential well depth
c_p	Porod constant
P	power law exponent

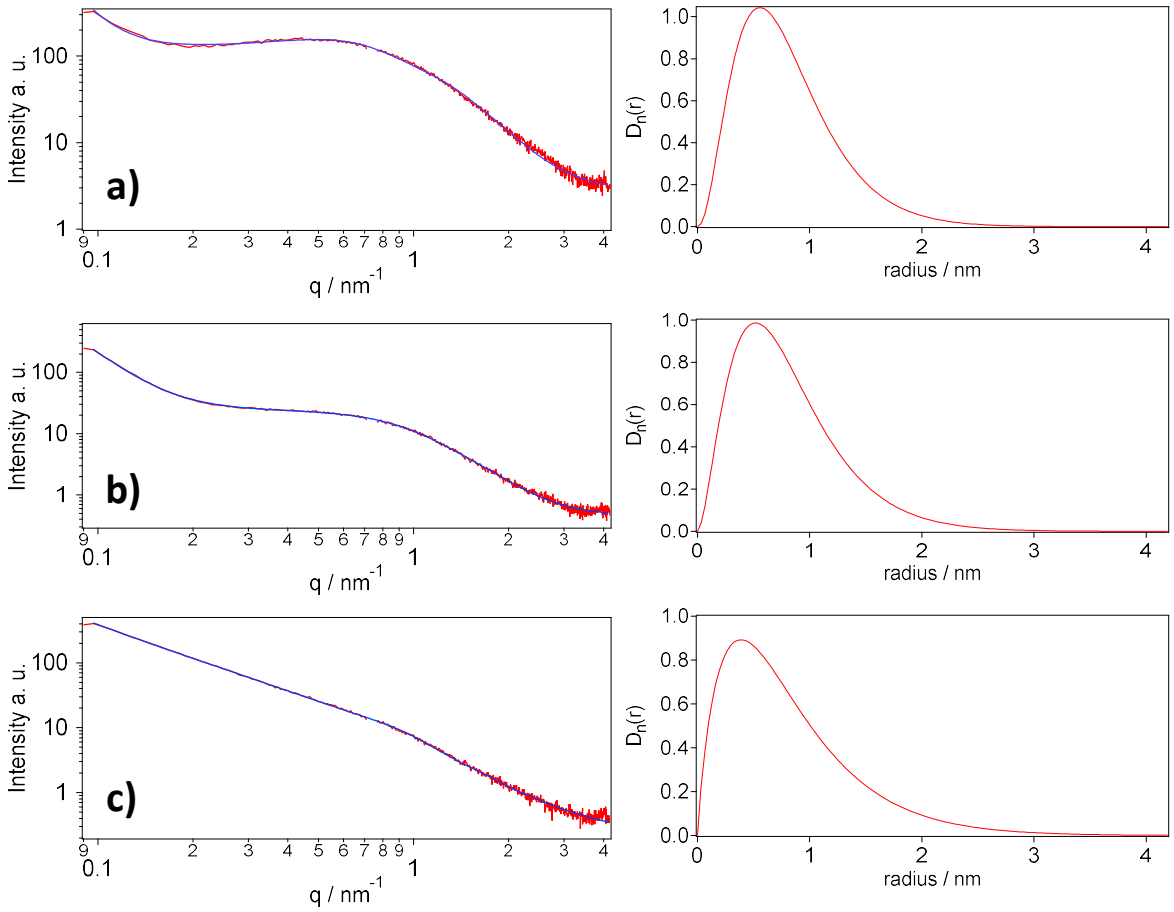

Fig. S18 *Line-cuts in the in-plane direction from the GISAXS heating runs (red line) after cooling down with the fitted pore-size distribution (blue-line) (left column) and the pore size distribution, calculated with the Schultz sphere distribution from the fitting function (right column): a) bulk DCM, b) bulk EDE and c) structured with 10 min O_2 plasma.*

Table S5 *Obtained fitting parameters for the fitting curves of Fig S17*

	back / a. u.	I_{sph} / a. u.	R_{sph} / nm	σ_{sph} / nm	R_{hs} / nm	p_{hs} / 1	ε_{hs} / k_bT	c_p	p
planar DCM	0.517	38.9	0.801	0.442	4.27	0.07	-0.397	$7*10^{-4}$	4.67
planar EDE	0.456	34.0	0.806	0.481	3.10	0.04	-0.273	0.02	3.98
structured EDE	0.159	25.0	0.818	0.593	3.81	$-5*10^{-4}$	420	3.11	2.04

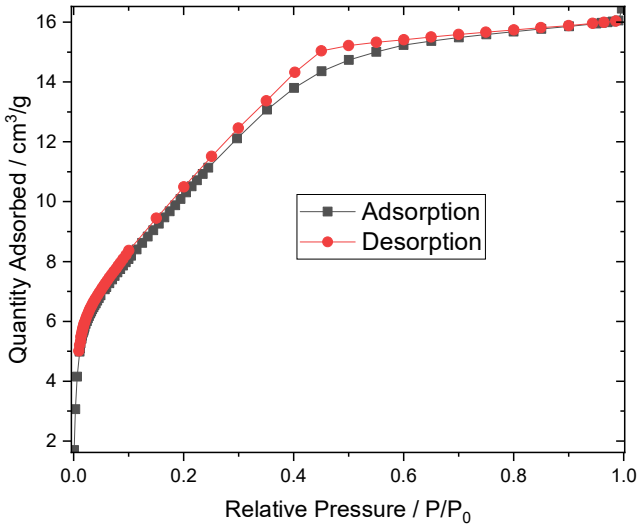

Fig. S19 *N_2 absorption and desorption of $ZnIn_2S_4$ powder.*

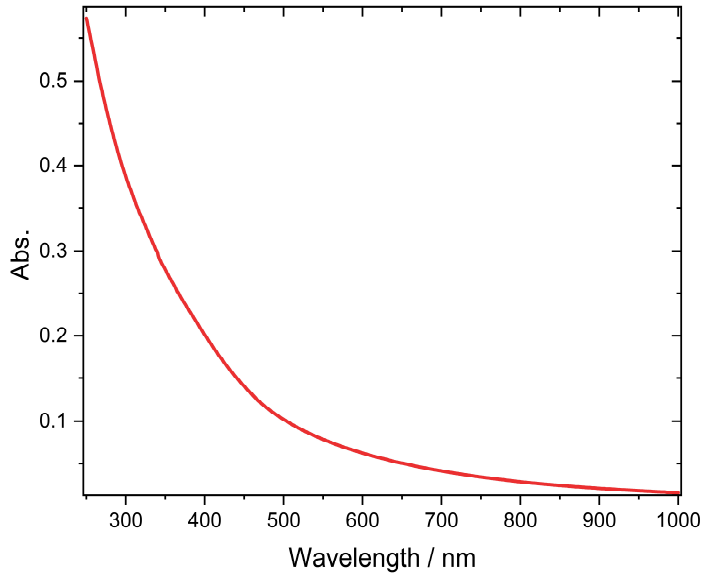

Fig. S20 *UV-Vis absorption spectrum of a $ZnIn_2S_4$ thin film on a CaF_2 substrate.*

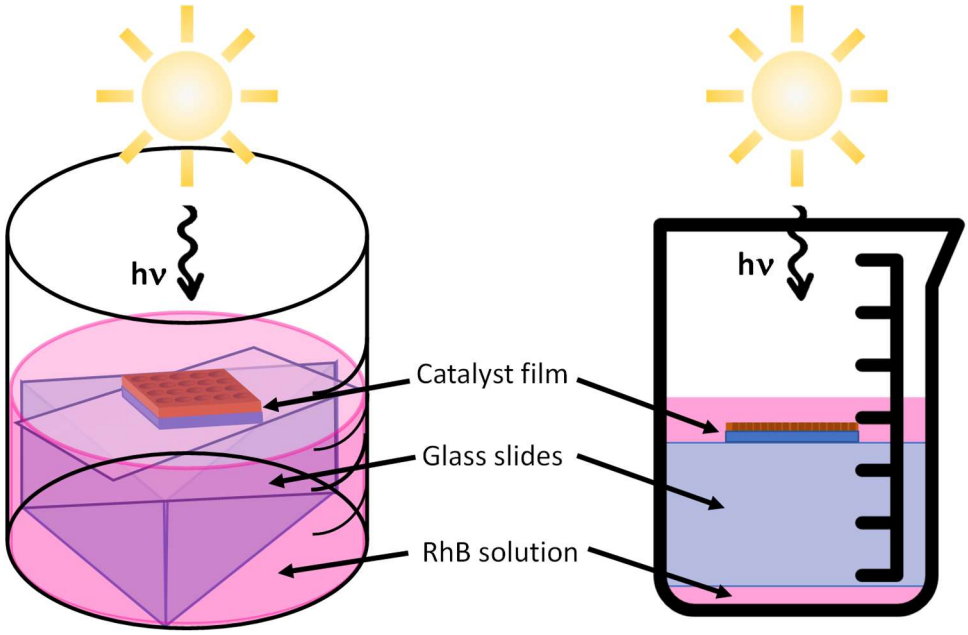

Fig. S21 *Set up for the photocatalytic dye degradation experiments.*

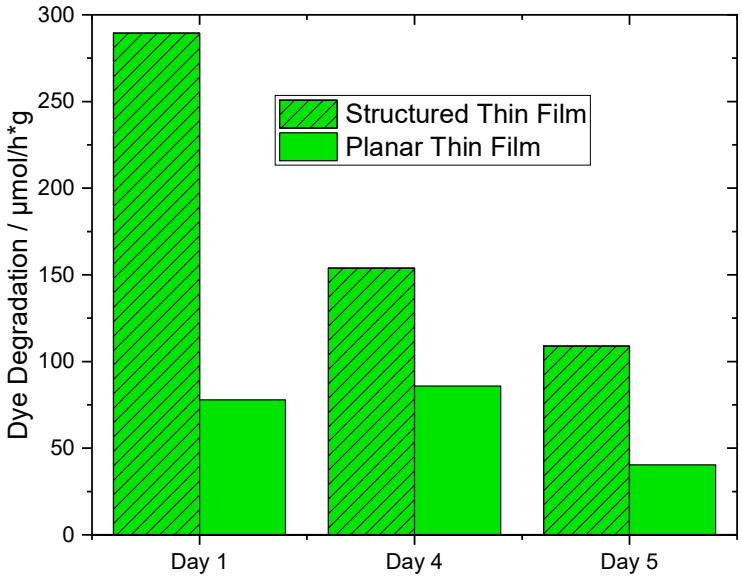

Fig. S22 *Catalytic activity in repeated catalytic dye degradation experiments over 5 days.*

Characterization

NMR spectra were measured with a Bruker Ultrashield 300 MHz NMR spectrometer. Solvent signals from the used solvents appeared at 7.26 ppm (1H, $CHCl_3$) and 4.79 ppm (H_2O). The spectra were evaluated with the Bruker software Topspin 3.1.

FTIR spectra were recorded on a Bruker Alpha FTIR spectrometer in ATR (attenuated total reflection) mode, employing a APLHA Platinum ATR single-reflection diamond ATR module and transmission mode. The spectra were recorded using 24 scans with air as background.

References

1 E. D. Campbell, *J. Am. Chem. Soc.*, 1900, **22**, 307–308.

2 T. Rath, M. Edler, W. Haas, A. Fischereder, S. Moscher, A. Schenk, R. Trattnig, M. Sezen, G. Mauthner, A. Pein, D. Meischler, K. Bartl, R. Saf, N. Bansal, S. A. Haque, F. Hofer, E. J. List and G. Trimmel, *Adv. Energy Mater.*, 2011, **1**, 1046–1050.

3 E. Vakalopoulo, T. Rath, M. Kräuter, A. Torvisco, R. C. Fischer, B. Kunert, R. Resel, H. Schröttner, A. M. Coclite, H. Amenitsch and G. Trimmel, *ACS Appl. Nano Mater.*, 2022, **5**, 1508–1520.

4 T. Ikeda and H. Hagihara, *Acta Cryst.*, 1966, **21**, 919–927.

5 T. C. Vagvala, S. S. Pandey, S. Krishnamurthy and S. Hayasa, *Z. Anorg. Allg. Chem.*, 2016, **642**, 134–139.

6 P. Liu, L. Bai, J. Yang, H. Gu, Q. Zhong, Z. Xie and Z. Gu, *Nanoscale Adv.*, 2019, **1**, 1672–1685.

7 E. Vakalopoulou, T. Rath, F. G. Warchomicka, F. Carraro, P. Falcaro, H. Amenitsch and G. Trimmel, *Mater. Adv.*, 2022, **3**, 2884–2895.

8 D. Pontoni, S. Finet, T. Narayanan and A. R. Rennie, *J. Chem. Phys.*, 2003, **119**, 6157–6165.

9 R. V. Sharma and K. C. Sharma, *Physica A*, 1977, **89**, 213–218.

10 M. Kotlarchyk, R. B. Stephens and J. S. Huang, *J. Phys. Chem.*, 1988, **92**, 1533–1538.

11 F. Rigodanza, M. Burian, F. Arcudi, L. Đorđević, H. Amenitsch and M. Prato, *Nat. Commun.*, 2021, **12**, 2640.